e-ISSN: 2687-4539
RESEARCH ARTICLE
Vol.7 / No.2 / 2025 / pp.117-124
https://doi.org/10.51537/chaos.1633880

Analog Circuit Implementation of Fractional-Order Modified Chua's Circuit

Burak Arıcıoğlu [*,β,1]
[*]Faculty of Technology, Electrical-Electronics Engineering, Sakarya University of Applied Sciences , Serdivan, Türkiye, [β]Biomedical Technologies Application and Research Center (Biyotam), Sakarya University of Applied Sciences, Serdivan, Türkiye.

ABSTRACT In this paper, the analog circuit implementation of a fractional-order chaotic system is presented. Fractionalization is achieved by replacing integer-order capacitors and inductors with their fractional-order counterparts in Chua's circuit. The paper provides a model for implementing fractional-order capacitors and inductors in the circuit. The results obtained from simulating the fractional-order Chua's circuit are compared with those derived from the Grünwald-Letnikov numerical solution. All results show strong agreement.

KEYWORDS
Chaos
Chaotic systems
Fractional-order systems
Chua's circuit
Circuit realization

INTRODUCTION

Chaos, as a science subject, was introduced by Edward Lorenz (Lorenz 1963). Later, Chua's circuit (Matsumoto 1984) became very important in the advancement of chaos science because it is the simplest autonomous chaotic circuit. In addition, when chaos was first introduced, few mathematical tools were available, so experimental methods were more favourable. In Chua's circuit, obtaining data experimentally is straightforward, which contributed to its widespread attention in the literature (Wu 1987).

In recent years, fractional-order chaos has become a topical subject because fractional-order chaotic systems exhibit richer dynamic behaviour than their integer order counterparts (Sheu *et al.* 2008). Numerous studies in the literature have explored the fractionalization of Chua's circuit. In most of these studies, only the system obtained from Chua's circuit is fractionalized mathematically without analog circuit implementation (Sene 2021; De la Sen *et al.* 2021; Boudjerida *et al.* 2022; Younis *et al.* 2025). Moreover, in some studies, Chua's circuit is fractionalized digitally so that it is implementation is carried out via a microcontroller (Wang *et al.* 2021; Wu *et al.* 2025) or an FPGA (field programable gate array) (Abd El-Maksoud *et al.* 2018; Wu *et al.* 2024; Abd El-Maksoud *et al.* 2019; Taşdemir *et al.* 2025).

Nowadays, there are numerous method implement chaotic system digitally (Emin and Yaz 2024; Kıran 2024; Seyyarer *et al.* 2025). However, in the analog realization, the system may exhibit more chaotic behaviour than in the digital realization because of the finite sampling intervals and precision (Michaels, A. J. 2011). Moreover, the analog circuit components are less complex and therefore much cheaper than digital circuit components.

This study aims to implement and validate an analog fractional-order Chua's circuit using fractional-order capacitors and inductors, comparing its behaviour with numerical simulations based on the Grünwald-Letnikov method. For the circuit implementation, a model for the fractional-order capacitor and inductor is introduced.

The main contribution of this study is the analog implementation of fractionalized Chua's circuit. The other main contribution is implementing fractional-order capacitor and inductor which are employed in many different study fields such as: control (Swain *et al.* 2017), fractional-order oscillators (Ahmad *et al.* 2001), fractional-order filters (Adhikary *et al.* 2016), fractional-order resonators (Adhikary *et al.* 2016), modelling of lithium-ion batteries (Zou, *et al.* 2017), modelling of neural networks (Peasgood *et al.* 2003) and so on.

The organization of the article is as follows. In the second section, the fractional-order operator and the modelling of the fractional-order capacitor and inductor is given. In the next section, fractional-order Chua's circuit are given. In the later section, the circuit implementation of the fractional-order Chua's circuit is presented. Finally, the conclusion is given in the last section.

Manuscript received: 5 February 2025,
Revised: 10 March 2025,
Accepted: 14 April 2025.

[1]baricioglu@subu.edu.tr (**Corresponding author**)

FRACTIONAL-ORDER CAPACITOR AND INDUCTOR

The Riemann–Liouville (RL) definition of fractional-order integrator is

$$ {}_0D_t^{-q} f(t) = \int_0^t \frac{(t-\tau)^{q-1}}{\Gamma(q)} f(\tau) d\tau \tag{1} $$

here q is the fractional-order. For a fractional-order capacitor, the relationship between the voltage and the current is

$$ v_C(t) = \frac{1}{C} {}_0D_t^{-q} i_C(t) = \frac{1}{C} \int_0^t \frac{(t-\tau)^{q-1}}{\Gamma(q)} i_C(\tau) d\tau \tag{2} $$

Here $v_C(t)$ is the voltage across the capacitor and $i_C(t)$ is the current passes through the capacitor. If we take the Laplace transform of Equation 2

$$ V_C(s) = \frac{1}{C} L\{{}_0D_t^{-q} i_c(t)\} = \frac{1}{C}\frac{1}{s^q} I_C(s) \tag{3} $$

From Equation 3 the impedance of the fractional-order capacitor obtained as

$$ Z_C(s) = \frac{V_C(s)}{I_C(s)} = \frac{1}{C}\frac{1}{s^q} \tag{4} $$

The impedance given in Equation 4 cannot be implemented using discrete components. However, its impedance function can be approximated as described in (Charef *et al.* 1992). This approximation is given in Equation 5

$$ \frac{1}{C}\frac{1}{s^q} \cong \frac{1}{C}\frac{1}{p_t^q}\frac{1}{\left(1+\frac{s}{p_t}\right)^q} \cong \frac{1}{C}\frac{1}{p_t^q}\frac{\prod_{i=0}^{N-1}\left(1+\frac{s}{z_i}\right)}{\prod_{i=0}^{N}\left(1+\frac{s}{p_i}\right)} \tag{5} $$

Here C is the capacitance of the fractional-order capacitor, q is the fractional-order, p_t is the corner frequency (alternatively $1/p_t$ is the relaxation time), and z_i, and p_i are the zeros and poles of the approximated impedance function respectively. The value of N in Equation 5 is calculated as (Charef *et al.* 1992)

$$ N = Integer\left(\frac{\log\left(\frac{w_{\max}}{p_0}\right)}{\frac{y}{10q(1-q)}}\right) + 1 \tag{6} $$

Also, the values of the poles and zeros of the approximated impedance function are calculated (Charef *et al.* 1992):

$$ \begin{aligned} p_0 &= p_t 10^{y/20q} \\ z_i &= (10^{y/10q(1-q)})^i 10^{y/10(1-q)} p_0 \\ p_i &= (10^{y/10q(1-q)})^i p_0 \end{aligned} \tag{7} $$

Here y is the maximum error in dB between the actual and the approximated lines. After all the poles and the zeros of the approximated impedance function are calculated, the partial fraction decomposition is performed to the right side of Equation 5.

$$ \frac{1}{C}\frac{1}{p_t^q}\frac{\prod_{n=0}^{N-1}\left(1+\frac{s}{z_i}\right)}{(s+p_o)(s+p_1)\ldots(s+p_N)} = \frac{r_0}{s+p_0} + \frac{r_1}{s+p_1} + \ldots + \frac{r_N}{s+p_N} \tag{8} $$

As seen in Equation 7, all the poles and zeros are in alternate order, hence all the residues in Equation 8 are positive constants. Because of this, the approximated impedance function can be implemented using passive elements. The simple fractions on the right side of Equation 8 can be easily realized by parallel connected RC elements. The value of the resistors and capacitors is calculated as:

$$ \begin{aligned} C_i &= \frac{1}{r_i} \\ R_i &= \frac{r_i}{p_i} \end{aligned} \tag{9} $$

The approximated impedance for the fractional-order capacitor is given in Figure 1.

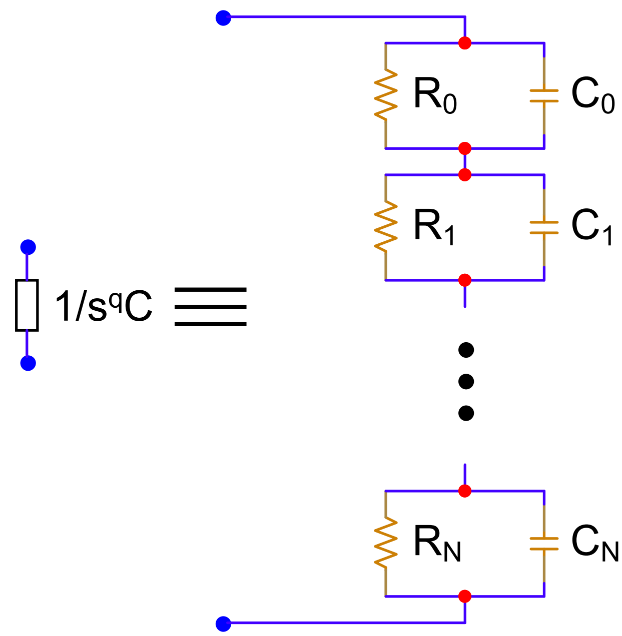

Figure 1 The approximated circuit for the fractional-order capacitor.

For a fractional-order induct-or, the relationship between the voltage and the current is

$$ v_L(t) = L_0 D_t^q i_L(t) = L\frac{1}{\Gamma(1-q)}\frac{d}{dt}\int_a^t \frac{i_L(\tau)}{(t-\tau)^q} d\tau \tag{10} $$

Here $v_L(t)$ is the voltage across the inductor and $i_L(t)$ is the current passes through the inductor. If we take the Laplace transform of Equation 10

$$ V_L(s) = L\, L\{{}_0D_t^q i_L(t)\} = Ls^q I_L(s) \tag{11} $$

From Equation 11 the admittance of the fractional-order inductor obtained as

$$ Y_L(s) = \frac{I_L(s)}{V_L(s)} = \frac{1}{L}\frac{1}{s^q} \tag{12} $$

The admittance given in Equation 12 cannot be implemented using discrete components. However, its admittance function can be approximated as described in (Charef *et al.* 1992). This approximation is given in Equation 13

$$ \frac{1}{L}\frac{1}{s^q} \cong \frac{1}{L}\frac{1}{p_t^q}\frac{1}{\left(1+\frac{s}{p_t}\right)^q} \cong \frac{1}{L}\frac{1}{p_t^q}\frac{\prod_{i=0}^{N-1}\left(1+\frac{s}{z_i}\right)}{\prod_{i=0}^{N}\left(1+\frac{s}{p_i}\right)} \tag{13} $$

Here L is the inductance of the fractional-order inductor, q is the fractional-order, p_t is the corner frequency (alternatively $1/p_t$ is the relaxation time), and z_i and p_i are the zeros and poles of the approximated admittance function respectively.

Here the value of N and, z_i, and p_i is calculated using Equation 6 and 7 respectively.

After all the poles and the zeros of the approximated admittance function are calculated, the partial fraction decomposition is performed to the right side of Equation 13.

$$\frac{1}{L}\frac{1}{p_t^q}\frac{\prod_{n=0}^{N-1}\left(1+\frac{s}{z_i}\right)}{(s+p_o)(s+p_1)\dots(s+p_N)}=\frac{r_0}{s+p_0}+\frac{r_1}{s+p_1}+\dots+\frac{r_N}{s+p_N} \tag{14}$$

As seen in Equation 7, all the poles and zeros are in alternate order, hence all the residues in Equation 14 are positive constants, too. This enables the implementation of the approximated admittance function using passive elements. The simple fractions on the right side of Equation 14 can be easily realized by series connected RL elements. The value of the resistors and inductors is calculated as:

$$\begin{aligned} L_i &= \frac{1}{r_i} \\ R_i &= \frac{p_i}{r_i} \end{aligned} \tag{15}$$

The approximated admittance for the fractional-order inductor is given in Figure 2.

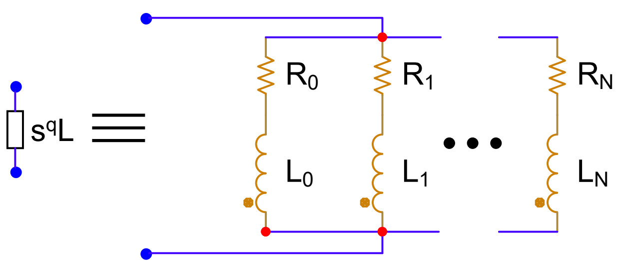

Figure 2 The approximated circuit for the fractional-order inductor.

FRACTIONAL-ORDER CHUA'S CIRCUIT

In this section, fractional-order Chua's circuit analysis is presented. The fractional-order Chua's circuit is given in Figure 3. In the modified version, only the nonlinear resistor (G_N) is changed as proposed by (Tang *et al.* 2003) with respect to the original circuit. In the modified version, the nonlinear resistor contains the $x|x|$ function instead of a piece-wise linear function.

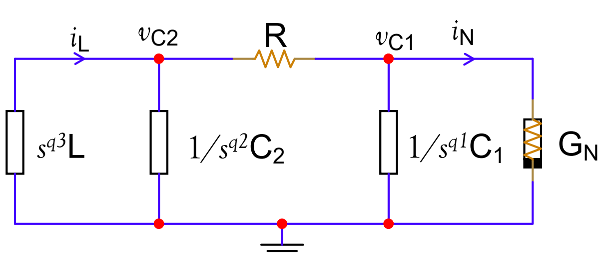

Figure 3 The fractional-order Chua's circuit.

For the modified nonlinear resistor, the voltage and current relationship is given in Equation 16.

$$i_N = g(v_N) = \alpha v_n + \beta v_n |v_n| \tag{16}$$

Here, i_N is the current passes through the nonlinear resistor and v_N is the voltage across the nonlinear resistor. As seen in Equation 16, the current of the nonlinear resistor is a function of the voltage.

If Kirchhoff's current law (KCL) is applied to the nodes v_{C1}, and v_{C2} the following fractional-order differential equation set is obtained.

$$\begin{aligned} C_1\,{}_0D_t^{-q_1} v_{C1} &= -\frac{v_{C1}-v_{C2}}{R} - g(v_{C1}) \\ C_2\,{}_0D_t^{-q_2} v_{C2} &= -\frac{v_{C2}-v_{C1}}{R} + i_L \\ L\,{}_0D_t^{-q_3} i_L &= -v_{C2} \end{aligned} \tag{17}$$

Then Equation 17 can be rewritten as:

$$\begin{aligned} {}_0D_t^{-q_1} v_{C1} &= -\frac{v_{C1}-v_{C2}}{RC_1} - \frac{1}{C_1}g(v_{C1}) \\ {}_0D_t^{-q_2} v_{C2} &= -\frac{v_{C2}-v_{C1}}{RC_2} + \frac{1}{C_2}i_L \\ {}_0D_t^{-q_3} i_L &= -\frac{1}{L}v_{C2} \end{aligned} \tag{18}$$

A fractional-order chaotic system can be obtained from Chua's circuit as in Equation 18. In the fractional-order chaotic system, the state variables are v_{C1}, v_{C2}, and i_L.

To investigate the dynamic behaviour of the fractional-order system, bifurcation diagrams and Lyapunov exponent analysis are carried out (Khan *et al.* 2025). In Fig. 4 bifurcation diagram is plotted with respect to the fractional-order q. In this bifurcation diagram, period doubling route to chaos is observed.

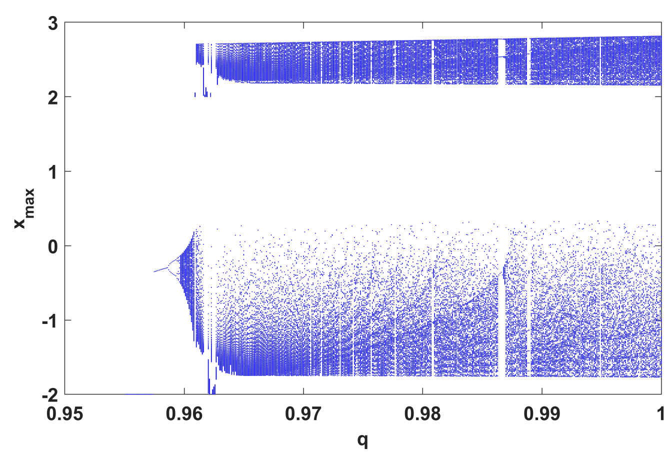

Figure 4 The bifurcation diagram with respect to the fractional-order q for the values of the circuit elements $R = 1, C_1 = 0.1079, C_2 = 1$, and $L = 0.0833$; and the initial conditions $v_{C1} = -1.01, v_{C2} = -0.01$, and $i_L = -0.01$.

Then, the bifurcation diagram is plotted with respect to the resistor R and shown in Fig. 5. In this bifurcation diagram, period doubling and period halving bifurcation is observed.

As a final dynamic analysis, the Lyapunov exponents are plotted and given in Fig. 6. As seen in Fig. 4, 5 and 6 the fractional-order system with given parameter values exhibits chaotic behaviour.

In this section, the numerical calculation of fractional-order Chua's circuit is also presented. For the numerical calculations, the

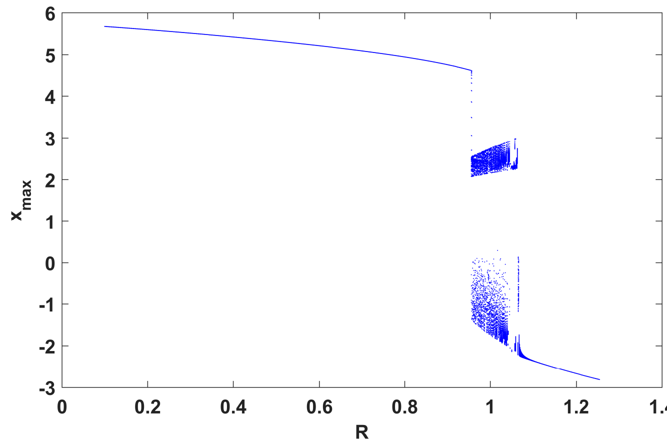

Figure 5 The bifurcation diagram with respect to the resistor R for the fractional-orders $q_1 = 0.96, q_2 = 0.97$, and $q_3 = 0.98$; the values of the circuit elements $C_1 = 0.1079, C_2 = 1$, and $L = 0.0833$; and the initial conditions $v_{C1} = -1.01, v_{C2} = -0.01$, and $i_L = -0.01$.

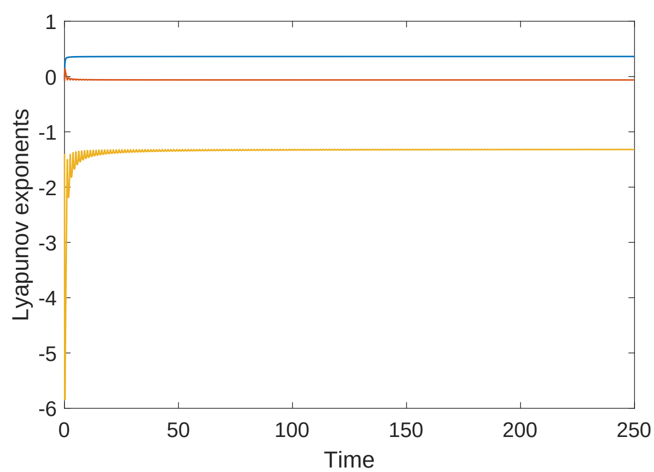

Figure 6 The Lyapunov exponents for the fractional-orders $q_1 = 0.96, q_2 = 0.97$, and $q_3 = 0.98$; the values of the circuit elements $R = 1, C_1 = 0.1079, C_2 = 1$, and $L = 0.0833$; and the initial conditions $v_{C1} = -1.01, v_{C2} = -0.01$, and $i_L = -0.01$.

Grünwald-Letnikov (GL) method is used since the finite difference-based definition of the GL is equivalent to the RL definition (Scherer *et al.* 2011; Chen *et al.* 2019).

Then, the fractional-order Grünwald–Letnikov fractional integral is:

$$ {}_0D_t^{-q} f(t) = \lim_{h \to 0} h^q \sum_{i=0}^{\frac{t}{h}} (-1)^i \binom{-q}{i} f(t - ih) \tag{19} $$

Here $f(t)$ is the differentiable function, q is the fractional-order, h is the step size, and $\binom{-q}{i}$ is the binomial coefficients.

In the numerical calculations the value of $R = 1$, $C_1 = 0.1079$, $C_2 = 1$, and $L = 0.0833$. Also, the values of parameters $\alpha = -1.5$ and $\beta = 0.25$, the initial conditions are selected as $v_{C1} = -1.01$, $V_{C2} = -0.01$, and $i_L = -0.01$ as given in (Wang *et al.* 2021). The voltage-current relationship graph of the nonlinear resistor is given in Figure 7. And the fractional-orders are selected as $q_1 = 0.96$, $q_2 = 0.97$, and $q_3 = 0.98$.

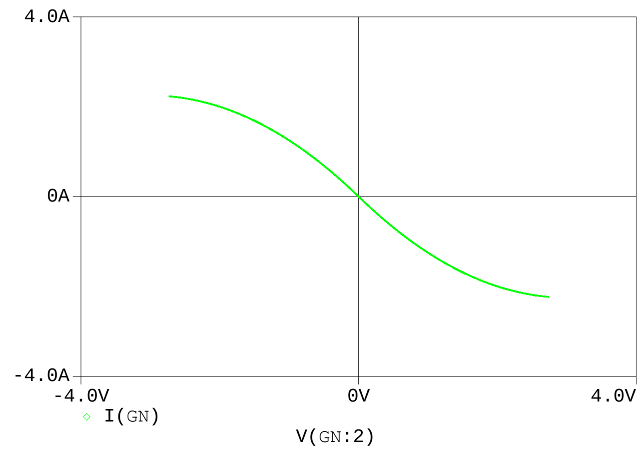

Figure 7 The voltage-current relationship of the nonlinear resistor .

For the given parameter values the fractional-order chaotic system in Equation 18 can be written as

$$ \begin{aligned} {}_0D_t^{-0.96} v_{C1} &= -9.267(v_{C1} - v_{C2}) - 9.267\left(-1.5v_{C1} + 0.25v_{C1}\,|v_{C1}|\right) \\ {}_0D_t^{-0.97} v_{C2} &= -\left(v_{C2} - v_{C1}\right) + i_L \\ {}_0D_t^{-0.98} i_L &= -12v_{C2} \end{aligned} \tag{20} $$

In Figure 8 the time series, in Figure 9 the phase portraits obtained from the numerical calculation are shown.

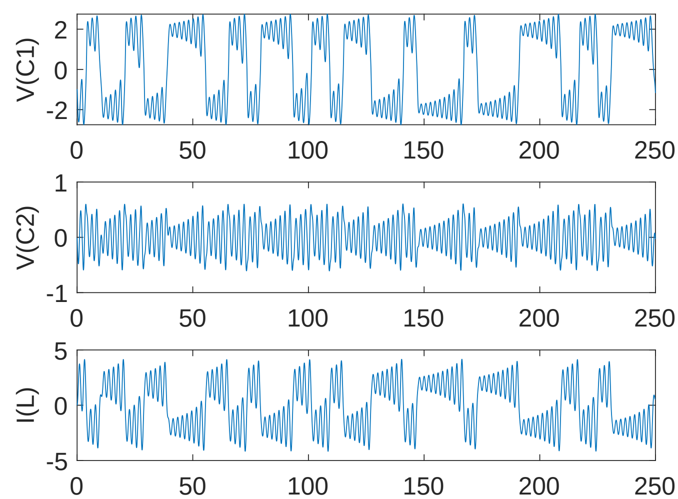

Figure 8 The time series of the fractional-order chaotic system when the fractional-orders $q_1 = 0.96, q_2 = 0.97$, and $q_3 = 0.98$; the values of the circuit elements $R = 1, C_1 = 0.1079, C_2 = 1$, and $L = 0.0833$; and the initial conditions $v_{C1} = -1.01, v_{C2} = -0.01$, and $i_L = -0.01$.

CIRCUIT IMPLEMENTATION

In this section, the circuit implementation of the fractional-order Chua's circuit and its simulation results are presented.

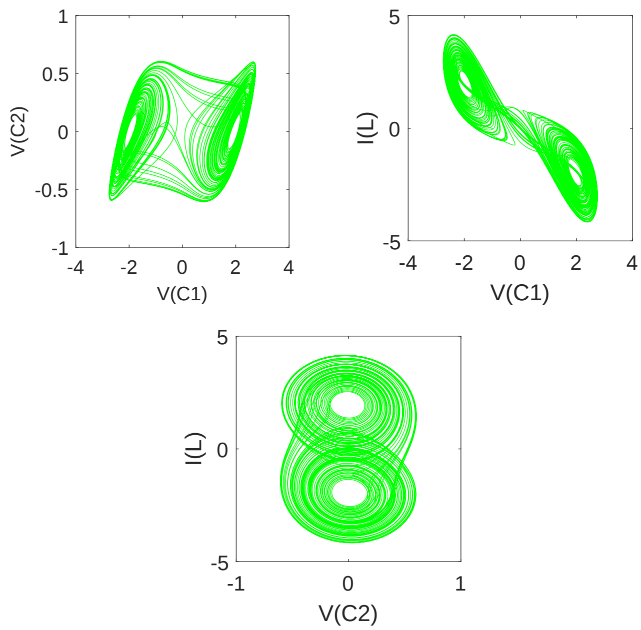

Figure 9 The phase portraits of the fractional-order chaotic system when the fractional-orders $q_1 = 0.96, q_2 = 0.97$, and $q_3 = 0.98$; the values of the circuit elements $R = 1, C_1 = 0.1079, C_2 = 1$, and $L = 0.0833$; and the initial conditions $v_{C1} = -1.01, v_{C2} = -0.01$, and $i_L = -0.01$.

In all the approximated impedance of admittance calculations, the maximum error $y = 0.3$ dB, the corner frequency $p_t = 0.01$rad/sec, and the maximum frequency $\omega_max = 100$ rad/sec.

For the fractional-order capacitor C_1 in Figure 3, the fractional-order is selected as $q_1 = 0.96$ and the value of $C_1 = 0.1079$F. For this case, the approximated impedance function has eight poles, and the values of the capacitors and resistors in the approximated impedance function are given in Table 1.

In Figure 10, the approximated and the actual impedance function is given for the frequency range of interest.

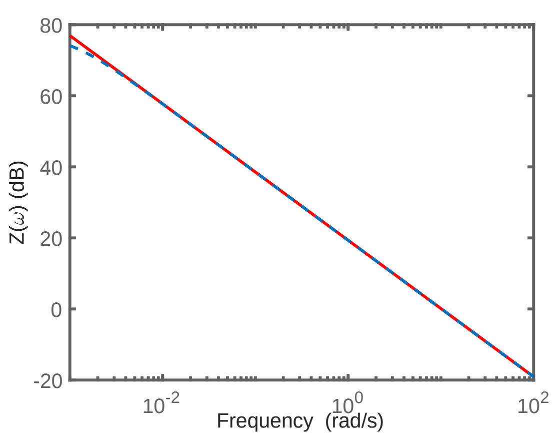

Figure 10 The approximated (blue dash) and the actual (red line) impedance function for the fractional-order capacitor C_1 over the frequency range of 0.001-100 rad/sec.

For the fractional-order capacitor C_2 in Figure 3, the fractional-order is selected as $q_2 = 0.97$ and the value of $C_2 = 1$F. For this case, the approximated impedance function has six poles, and the values of the capacitors and resistors in the approximated impedance function are given in Table 2.

In Figure 11, the approximated and the actual impedance function is given for the frequency range of interest.

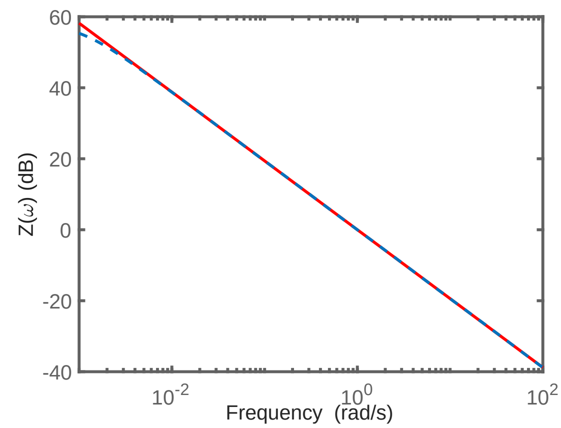

Figure 11 The approximated (blue dash) and the actual (red line) impedance function for the fractional-order capacitor C_2 over the frequency range of 0.001-100 rad/sec.

For the fractional-order inductor L in Figure 3, the fractional-order is selected as $q_3 = 0.98$ and the value of $L = 0.0833$H. For this case, the approximated admittance function has five poles, and the values of the inductors and resistors in the approximated admittance function are given in Table 3.

In Figure 12, the approximated and the actual admittance function is given for the frequency range of interest.

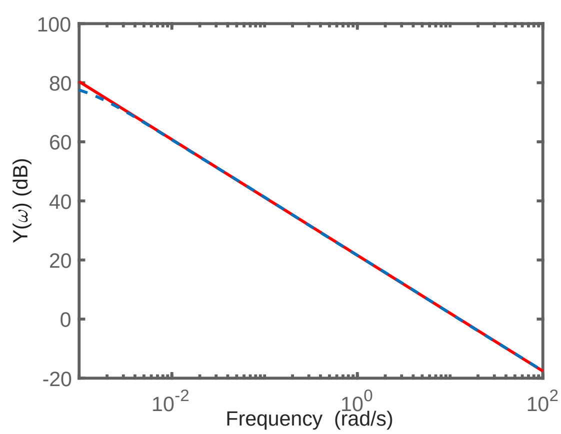

Figure 12 The approximated (blue dash) and the actual (red line) admittance function for the fractional-order inductor L over the frequency range of 0.001-100 rad/sec.

In Figure 13, the complete circuit for the fractional-order Chua's circuit is shown. The nonlinear resistor is modelled with an analog behaviour model (ABM) device in Spice

The time series and the phase portraits obtained from the simulation of the fractional-order Chua's circuit are shown in Figure 14 and 15, respectively.

Table 1 **The values of capacitors and resistors for the approximation of fractional-order capacitor C_1 in Figure 3.**

n	0	1	2	3	4	5	6	7
C_i(F)	0.140	1.562	1.671	1.588	1.483	1.381	1.282	1.175
$R_i(\Omega)$	6908.38	102.21	15.81	2.75	0.488	0.0867	0.0155	0.0028

Table 2 **The values of capacitors and resistors for the approximation of fractional-order capacitor C_2 in Figure 3.**

n	0	1	2	3	4	5
C_i(F)	1.197	14.709	14.868	13.947	12.989	12.005
$R_i(\Omega)$	806.10	6.11	0.563	0.0559	0.0056	0.0006

Table 3 **The values of capacitors and resistors for the approximation of fractional-order capacitor C_2 in Figure 3.**

n	0	1	2	3	4
L_i(H)	0.093	1.230	1.178	1.099	1.022
$R_i(\Omega)$	0.0001	0.043	1.40	44.46	1402.82

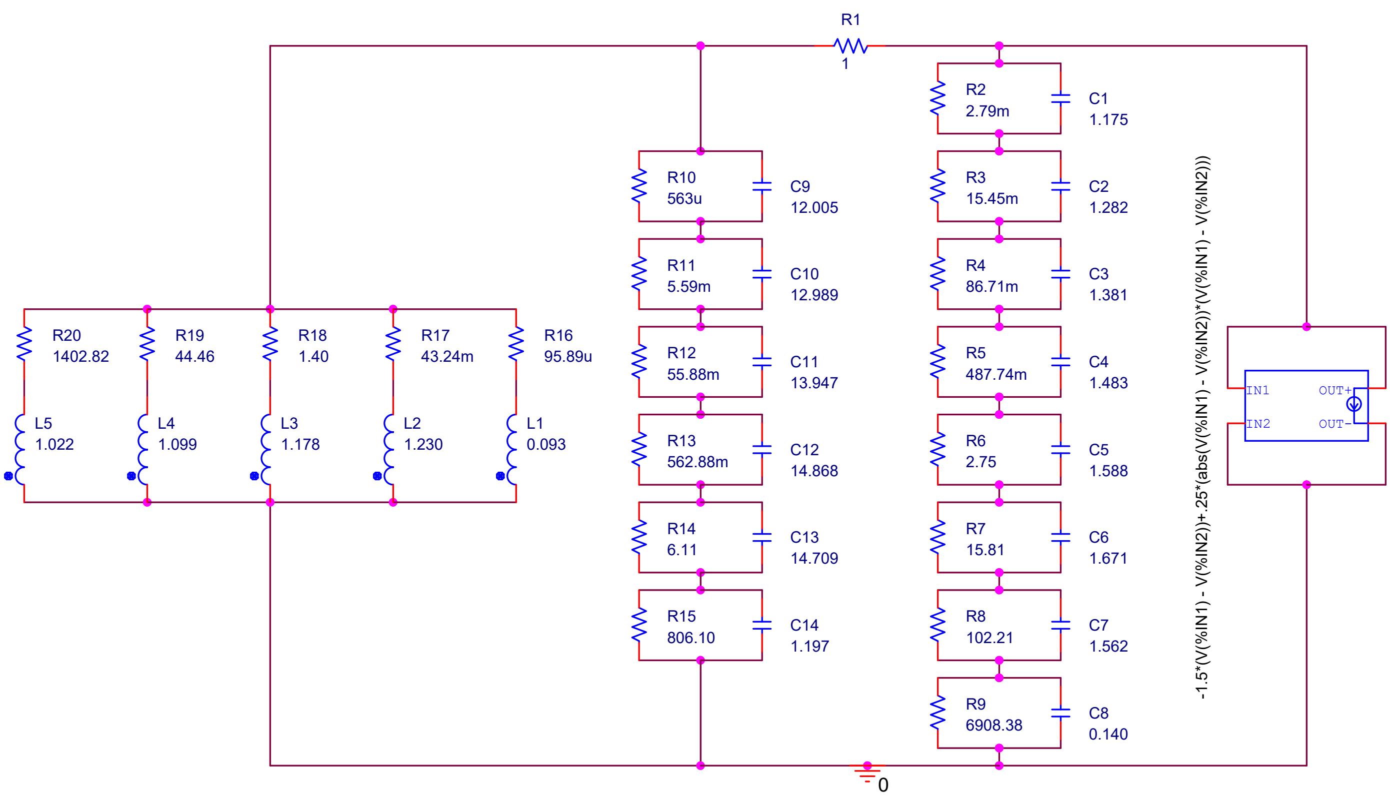

Figure 13 The circuit implementation of the fractional-order Chua's circuit when the fractional-orders $q_1 = 0.96, q_2 = 0.97$, and $q_3 = 0.98$; the values of the circuit elements $R = 1, C_1 = 0.1079, C_2 = 1$, and $L = 0.0833$.

As seen in Figure 8, 9,14, and 15, the time series and the phase portraits obtained from numeric calculation and simulation are very close to each other. This shows that the fractional-order Chua's circuit is realized successfully. In addition, the modelling of fractional-order capacitor, and inductor is accurate enough.

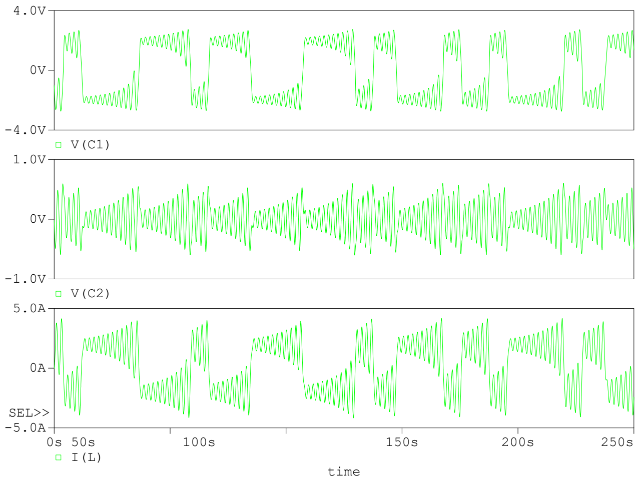

Figure 14 The time series of the fractional-order Chua's circuit when the fractional-orders $q_1 = 0.96, q_2 = 0.97$, and $q_3 = 0.98$; the values of the circuit elements $R = 1, C_1 = 0.1079, C_2 = 1$, and $L = 0.0833$; and the initial conditions $v_{C1} = -1.01, v_{C2} = -0.01$, and $i_L = -0.01$.

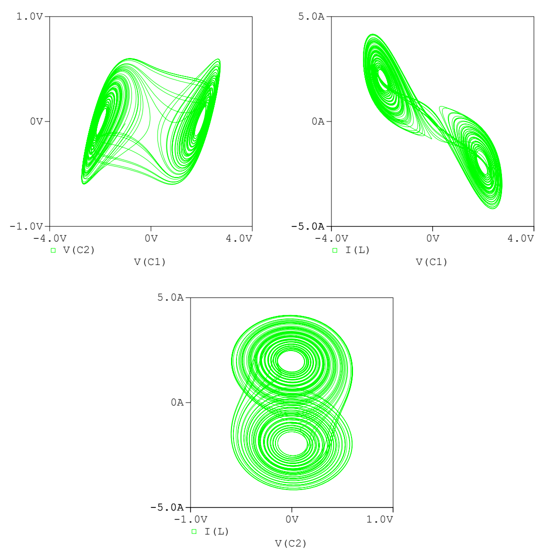

Figure 15 The phase portraits of the fractional-order Chua's circuit when the fractional-orders $q_1 = 0.96, q_2 = 0.97$, and $q_3 = 0.98$; the values of the circuit elements $R = 1, C_1 = 0.1079, C_2 = 1$, and $L = 0.0833$; and the initial conditions $v_{C1} = -1.01, v_{C2} = -0.01$, and $i_L = -0.01$

CONCLUSION

In this study, Chua's circuit is fractionalized by using fractional-order capacitors and an inductor. By applying the circuit analysis to the fractionalized Chua's circuit, a fractional-order chaotic system is obtained and is solved numerically with the GL algorithm. Then, the analog realization of the fractional-order Chua's circuit is successfully implemented. In the paper, it is shown that the numerical and simulation results are in good accordance. This is one of the main contributions of the paper, since in most of the studies Chua's circuit is fractionalized either numerically or digitally. Another contribution is that the paper presents modelling of fractional-order capacitor and inductor. For the presented method to be applicable for the modelling of the fractional-order capacitor and inductor, the fractional-order must vary between 0 and $1 (0 < q < 1)$. Final remark, there is no direct method for determining the value of maximum error y and the frequency range other than trial and error.

Ethical standard

The author has no relevant financial or non-financial interests to disclose.

Availability of data and material

Not applicable.

Conflicts of interest

The author declares that there is no conflict of interest regarding the publication of this paper.

LITERATURE CITED

Abd El-Maksoud, A. J., A. A. Abd El-Kader, B. G. Hassan, M. A. Abdelhamed, N. G. Rihan, *et al.*, 2018 FPGA implementation of fractional-order Chua's chaotic system. In *2018 7th international conference on modern circuits and systems technologies (MOCAST)*, (pp. 1–4), IEEE.

Abd El-Maksoud, A. J., A. A. Abd El-Kader, B. G. Hassan, N. G. Rihan, M. F. Tolba, *et al.*, 2019 FPGA implementation of sound encryption system based on fractional-order chaotic systems. Microelectronics Journal **90**: 323–335.

Adhikary, A., S. Sen, and K. Biswas, 2016 Practical realization of tunable fractional order parallel resonator and fractional order filters. IEEE Transactions on Circuits and Systems I: Regular Papers **63(8)**: 1142–1151.

Ahmad, W., R. El-Khazali, and A. S. Elwakil, 2001 Fractional-order Wien-bridge oscillator. Electronics Letters **37(18)**: 1110–1112.

Boudjerida, N., M. S. Abdelouahab, R. Lozi, 2022 Modified projective synchronization of fractional-order hyperchaotic memristor-based Chua's circuit. Journal of Innovative Applied Mathematics and Computational Sciences **2(3)**: 69–85.

A. Charef, H. H. Sun, Y. Y. Tsao, and B. Onaral, 1992 Fractal system as represented by singularity function. IEEE Transactions on automatic Control **37(9)**: 1465–1470.

H. Chen, F. Holland, and M. Stynes, 2019 An analysis of the Grünwald-Letnikov scheme for initial-value problems with weakly singular solutions. Applied Numerical Mathematics **139**: 52–61.

De la Sen, M., S. Deniz, and H. Sözen, 2021 A new efficient technique for solving modified Chua's circuit model with a new fractional operator. Advances in Difference Equations **2021**: 1–16.

Emin, B., and M. Yaz, 2024 Digital Implemen-tation of Chaotic Systems Using Nvidia Jetson AGX Orin andCustom DAC Converter. Chaos and Fractals **1(1)**: 38–41.

Khan A., C. Li, Z. Zhang, and X. Cen, 2025 ATwo-memristor-based Chaotic System with Symmetric Bifurcationand Multistability. Chaos and Fractals **2(1)**: 1–7.

Kiran, H. E., 2025 A Novel Chaos-Based Encryp-tion Technique with Parallel Processing Using CUDA for MobilePowerful GPU Control Center. Chaos and Fractals **1(1)**: 6–18.

Lorenz, E. N., 1963 Deterministic nonperiodic flow. Journal of atmospheric sciences **20(2)**: 130–141.

Matsumoto, T., 1984 A chaotic attractor from Chua's circuit. IEEE transactions on circuits and systems **31(12)**: 1055–1058.

Michaels, A. J., 2011 Quantitative comparisons of digital chaotic circuits for use in communications. In *roceedings of the Joint INDS 11 & ISTET 11*, (pp. 1–8), IEEE.

Peasgood, W., L. A. Dissado, C. K. Lam, A. Armstrong, and W. Wood, 2003 A novel electrical model of nerve and muscle using Pspice. Journal of Physics D: Applied Physics **36(4)**: 311.

Scherer, R., S.L. Kalla, Y. Tang, and J. Huang, 2011 The Grünwald-Letnikov method for fractional differential equations. Computers & Mathematics with Applications **62(3)**: 902–917.

Sene, N., 2021 Mathematical views of the fractional Chua's electrical circuit described by the Caputo-Liouville derivative. Revista mexicana de fisica **67(1)**: 91–99.

Seyyarer, E., F. Ayata, and S. Özdem, 2025 The Role of Technological Approaches in Cyber Security of Au-tonomous Vehicles. ADBA Computer Science **2(1)**, 1–6.

Sheu, L. J., H.K. Chen, J. H. Chen, L. M. Tam, W. C. Chen, *et al.*, 2008. Chaos in the Newton-–Leipnik system with fractional order. Chaos, Solitons & Fractals **36(1)**: 98–103.

Swain, S. K., D. Sain, S. K. Mishra, and S. Ghosh, 2017 Real time implementation of fractional order PID controllers for a magnetic levitation plant. AEU-International Journal of Electronics and Communications **78**: 141–156.

Tang, K. S., K. F. Man, G. Q. Zhong, and G. Chen, 2003 Modified Chua's circuit with $x|x|$. Control Theory and Application **20**: 223–227.

Taşdemir, M. F., M. Tuna, and I. Koyuncu, 2025 FPGA-Based Chaotic Oscillator Designs and Performance Analysis. Chaos and Fractals **2(1)**, 8–13.

Wang, J., L. Xiao, K. Rajagopal, A. Akgul, S. Cicek, and B. Aricioglu, 2021 Fractional-order analysis of modified Chua's circuit system with the smooth degree of 3 and its microcontroller-based implementation with analog circuit design. Symmetry **13(2)**: 340.

Wu, C., L. Xiong, and N. Yang, 2024 Modeling and dynamics analysis of a novel fractional-order meminductive multi-stable chaotic circuit and its FPGA implementation. Chaos, Solitons & Fractals **186**: 115222.

Wu, S., 1987 Chua's circuit family. Proceedings of the IEEE **75(8)**: 1022–1032.

Wu, X., K. Hu, S. He, H. Wang, and Z. Zhang, 2025 A fractional-order Chua's system: System model, numerical simulations, hidden dynamics, DSP implementation and voice encryption application. AEU-International Journal of Electronics and Communications 155691.

Younis, M., H. Ahmad, M. Ozturk, and D. Singh, 2025 A novel approach to the convergence analysis of chaotic dynamics in fractional order Chua's attractor model employing fixed points. Alexandria Engineering Journal **110**: 363–375.

Zou, C., X. Hu, S. Dey, L. Zhang, and X. Tang, 2017 Nonlinear fractional-order estimator with guaranteed robustness and stability for lithium-ion batteries. IEEE Transactions on Industrial Electronics **65(7)**: 5951–5961.

How to cite this article: Arıcıoğlu, B. Analog Circuit Implementation of Fractional-Order Modified Chua's Circuit. *Chaos Theory and Applications*, 7(2), 117-124, 2025.